Answers to Anonymous Referee 1 on the paper 'Does the rotational direction of a wind turbine impact the wake in a stably stratified atmospheric boundary layer?'

Englberger et al.

A.Simulations

A1

The inflow conditions need to be added to the text, specifically, profiles of stream wise and lateral wind, temperature, turbulence intensities (in different directions) and Reynolds shear stresses, as these parameters would affect the wake aerodynamics.

The profiles of u and v are given in Eqs. 4 and 5. We forget to mention the potential temperature profile, we added it now as: 'The potential temperature is

$$\Theta_{BL}(z) = \frac{3\,K}{200\,m} z \tag{1}$$

in the lowest 200 m and 303 K above. '

As they are idealized profiles we think it is not mandatory to show them in a plot. The turbulence intensity is discussed in detail in Englberger and Dörnbrack (2018a), we cited the reference in the paper.

The Reynolds stress tensor terms $u'u'$, $w'w'$, and $u'w'$ are exactly the same in NV and V simulations. As we discuss the differences in the wake in this paper, which only depend on the differences between V and NV and not on individual values, we decided to add a figure in the paper showing the relevant differences of lateral wind and Reynolds stresses:

a the incoming wind v and the incoming wind direction ϕ in Fig. 2(a)

b the Reynolds stress tensor terms $u'v'$ and $v'v'$ (and $v'w'$ with only minor differences) in Fig. 2(b)

Representing only the differences between V and NV is further helpful to understand the differences in the flow rotation plot outside the rotor (Fig. 10 and 11).

It is included in the text as:

a 'The differences in the inflow conditions between veered and non-veered simulations are presented in Fig. 2(a) for the spanwise velocity v and the wind direction with respect to 270 ° as V - NV.'

b 'The ABL flow (Eqs. 4-8) in combination with the impressed turbulence of a stably stratified regime result in exactly the same Reynolds stress tensor terms of $u'u'$, $w'w$, and $u'w'$ in V and NV whereas there are differences in $v'v'$, $u'v'$, and

$v'w'$ (Fig. 2(b)). In the height of the rotor, $u'v'$ is symmetric with respect to hub height and both $u'v'$ and $v'v'$ increase approaching the blade tip, whereas $v'w'$ is marginal.'

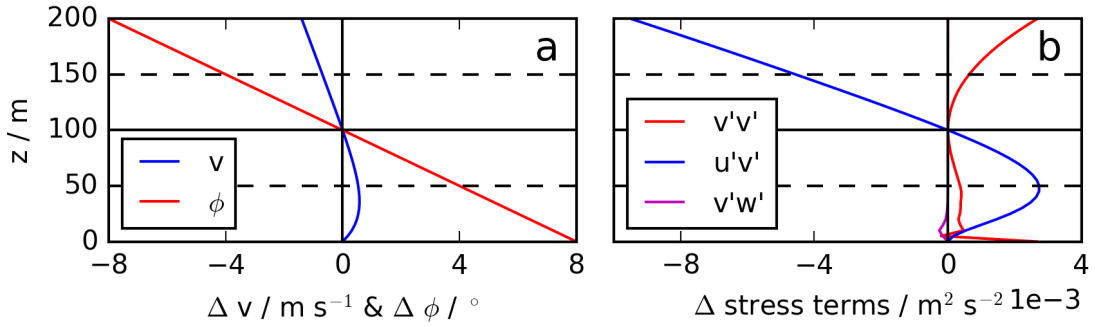

Figure 1. Differences in the initial conditions between V and NV for the spanwise velocity v and the incoming wind direction ϕ, whereas the differences are related to 270°, in (a) and the Reynolds stress tensor terms $v'v'$, $u'v'$ and $v'w'$ in (b).

A2

It is mentioned that the turbulence intensity is the same in no-veer and veering cases. Is it turbulence intensity in the streamwise direction or the total turbulence level? As the other terms in the Reynolds stress tensor also contribute to the turbulent transport and the wake recovery, would it be enough to match the turbulence level in no-veer and veering cases?

See A1. We additionally discussed and plotted the Reynolds stress tensor terms.

A3

In veering inflow simulation, the wind direction changes with height, and it might also change with time. Is the wind direction fixed during the simulation?

In the simulations, the wind direction changes only with height, they are fixed with time.

How the wind direction is kept constant during the simulation to avoid any yaw misalignment?

We verify a constant wind direction by applying the Eqs. 4, 5, and 7 of $u_{BL}(z)$, $v_{BL}(z)$, and $w_{BL}(z)$. This results in $v(hub) = 0$ all the time. The applied parametrization of Englberger and Dörnbrack (2018b) verifies no positive or negative tendency of v at each height for the considered 10 min averaging time. Therefore, the flow is directly perpendicular to the nacelle at hub height and symmetric in the lower and the upper rotor part.

A4

What is the rotational speed of the turbine and how it is set during the simulations – with and without wind veer? The main characteristics of the turbine such as turbine RPM, turbine thrust and power coefficients should be added to the text for different

cases.

The rotational speed of the turbine is fixed at 7 rpm in all simulations. We added the value in the description of the wind-turbine parametrization. 'Further, the rotation frequency Ω is set to 7 rpm.'

As we apply the BEM method, we do not have a constant c_T or c_P value. However, we cited the turbine, we used for the parametrization of the BEM method.

A5

Based on the domain size, the blockage ratio is about 8% which is relatively large for simulations of a stand-alone wind turbine. It is recommended that the blockage ratio should be less than 2% to neglect its effect on wake development. Please clarify this point.

As blockage is relevant for confined simulations, it should not be relevant for this work as we present open boundary condition simulations.

A6

The authors mentioned that the simulations are performed for 20 minutes and the results are averaged over the last 10 minute. Is 10min enough for the averaging? I believe a longer time should be considered for averaging especially for far wake region to make sure the statistics are well converged.

In Englberger and Dörnbrack (2018a) we investigated the effect of the time used for averaging resulting that under moderately and strongly stably stratified (SBL and MBL) conditions, the 10 min, 30 min and 50 min averages result in an almost identical turbulent intensity profile. In contrast, it was found that under convective and near-neutral (CBL and EBL) stratifications, a longer averaging period of at least 30 min is necessary. Therefore, the considered SBL case resulting from the same diurnal cycle precursor simulation from Englberger and Dörnbrack (2018a) shows that an averaging time of 10 min is enough.

I think the full recovery of the wake occurred at 16D might be related to limited simulation time.

We are not sure why the reviewer suggests a full wake recovery at 16 D, according to Figs. 4, 5, and 6 this is not the case for $x < 20$ D.

B. Interpretation of the results

We agree with the Reviewer and included vertical and spanwise profiles including velocity and turbulent intensity information at 10 D downstream to allow a more quantitative comparison between the three considered veered cases.

B1

All the results are qualitative, and the paper suffers from the lack of quantitative comparisons. Velocity profiles at different distances from the turbine need to be plotted and added to the text to better quantified the effect of wake rotation.

We added vertical and spanwise profiles presenting the difference in velocity deficit ΔVD between each two of the discussed

simulations in the paper (Figs. 2 (a, c, e, g) and 3 (a, c, e, g)). We decide not to include a plot showing the exact values of vertical and horizontal profiles of u for all six simulations (as tested in Fig. 4), as showing ΔVR is much more representative, the difference is much easier to see and further the individual figures are not of major interest as it is an idealized study.

B2

In the text, the analysis is only focused on the mean velocity (first-order statistics). Why only the mean velocity? How does the wake rotation affect the turbulence level or TKE behind the turbine in a stable regime?

See B1 part and Figs. 2 (b, d, f, h) and 3 (b, d, f, h).

B3

The authors use a fixed value for the wind veer (0.08 deg/m). What would be the effect of wind veer strength (or rotor size) on the results? As the effect of wind veer has been extensively studied before, it is expected that a more comprehensive investigation to be done.

The impact of the strength of wind veer and also the rotor position affected by veer (upper or lower rotor half or full rotor as in this study) is a very interesting topic, and is discussed in detail in two further publications, one will be published in the next days Englberger and Lundquist (2019) and on will be submitted within in the next weeks Englberger et al. (2019). The wind veer strength has an impact on the difference between wake veer and inflow wind veer. This difference decreases if the vertical gradient of the veering wind increases (Englberger and Lundquist, 2019). Further, a larger vertical gradient of the veering wind decreases the wake difference induced by the rotational direction (Englberger et al., 2019). We did not add it in this work, as it is a rather complex issue, with additional parameters impacting the wake difference.

The rotor size is not changed. However, changing the amount of deg/m should be comparable to a constant wind veer value while changing the rotor diameter. Both would result in the same amount of wind veer over the whole rotor.

B4

In page 9, line 3: the authors mentioned that: “this enhanced production of TKE due to the shear and wind veer . . ..” The authors did not show any results about the TKE or TKE production in the text. It is not clear how they concluded that TKE production increases due to the veer.

We added TKE now to the paper (see B2).

B5

Following the previous comments, it would be useful that the authors show how the wake rotation can affect the TKE production in the wake.

We added TKE now to the paper (see B2).

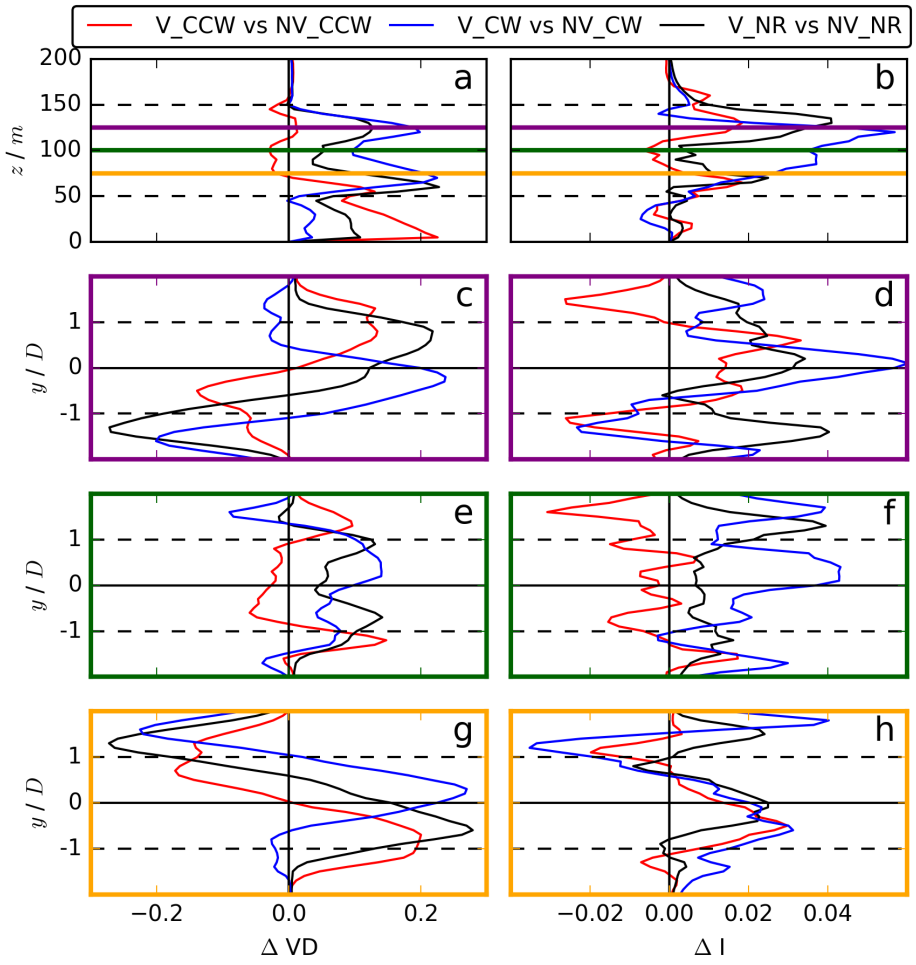

Figure 2. Vertical and spanwise profiles of ΔVD in (a), (c), (e), (g) and ΔI in (b), (d), (f), (h) at 10 D. The spanwise profiles are plotted at 75 m (orange frame, (g), (h)), 100 m (hub height) (green frame, (e) (f)), and 125 m (purple frame (c), (d)). In panels (a) and (b), the coloured lines indicate the altitudes analysed in (c) - (h). Considering a comparison of two simulations A and B (see legend: A vs B), ΔVD is calculated as the difference between simulation B and simulation A $VD(B) - VD(A)$ and ΔI as the difference between simulation A and simulation B $I(A) - I(B)$. Therefore, $\Delta VD > 0$ and likewise $\Delta I > 0$ represent a more rapid wake recovery of simulation A in comparison to simulation B, related to a higher turbulence intensity level.

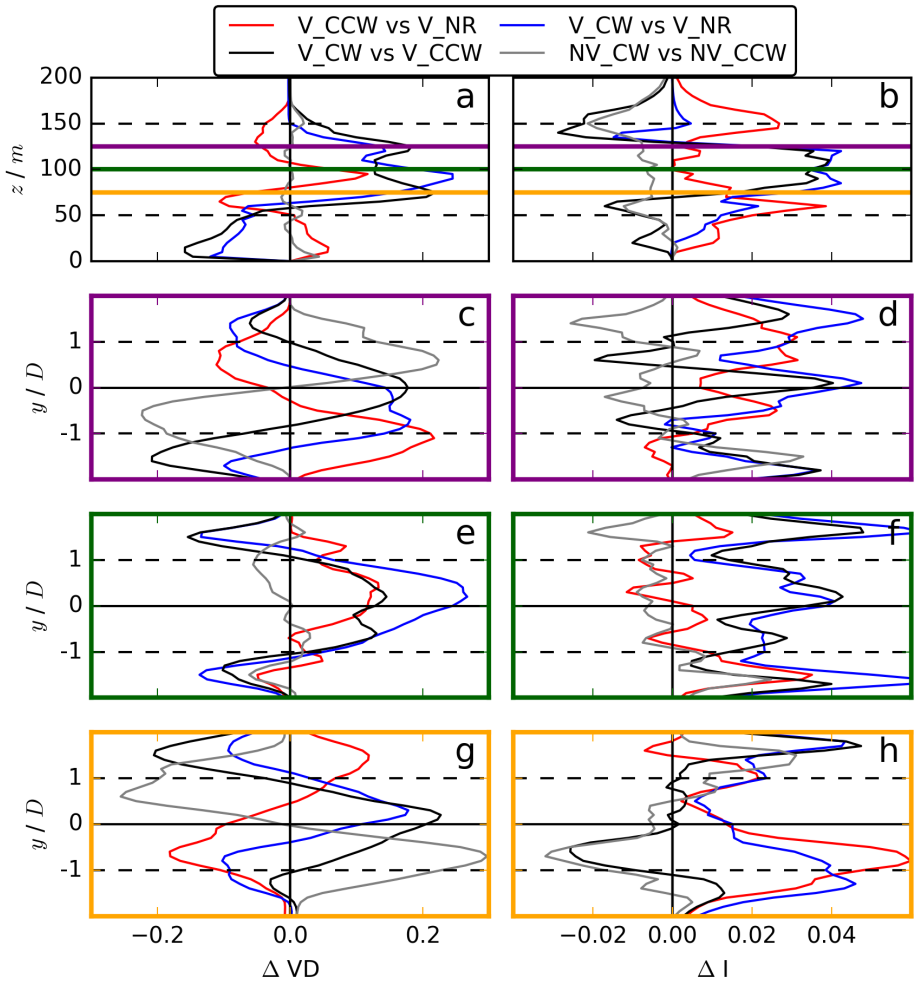

Figure 3. Vertical and spanwise profiles of ΔVD in (a), (c), (e), (g) and ΔI in (b), (d), (f), (h) at 10 D. The spanwise profiles are plotted at 75 m (orange frame, (g), (h)), 100 m (hub height) (green frame, (e) (f)), and 125 m (purple frame (c), (d)). In panels (a) and (b), the coloured lines indicate the altitudes analysed in (c) - (h). Considering a comparison of two simulations A and B (see legend: A vs B), ΔVD is calculated as the difference between simulation B and simulation A $VD(B) - VD(A)$ and ΔI as the difference between simulation A and simulation B $I(A) - I(B)$. Therefore, $\Delta VD > 0$ and likewise $\Delta I > 0$ represent a more rapid wake recovery of simulation A in comparison to simulation B, related to a higher turbulence intensity level.

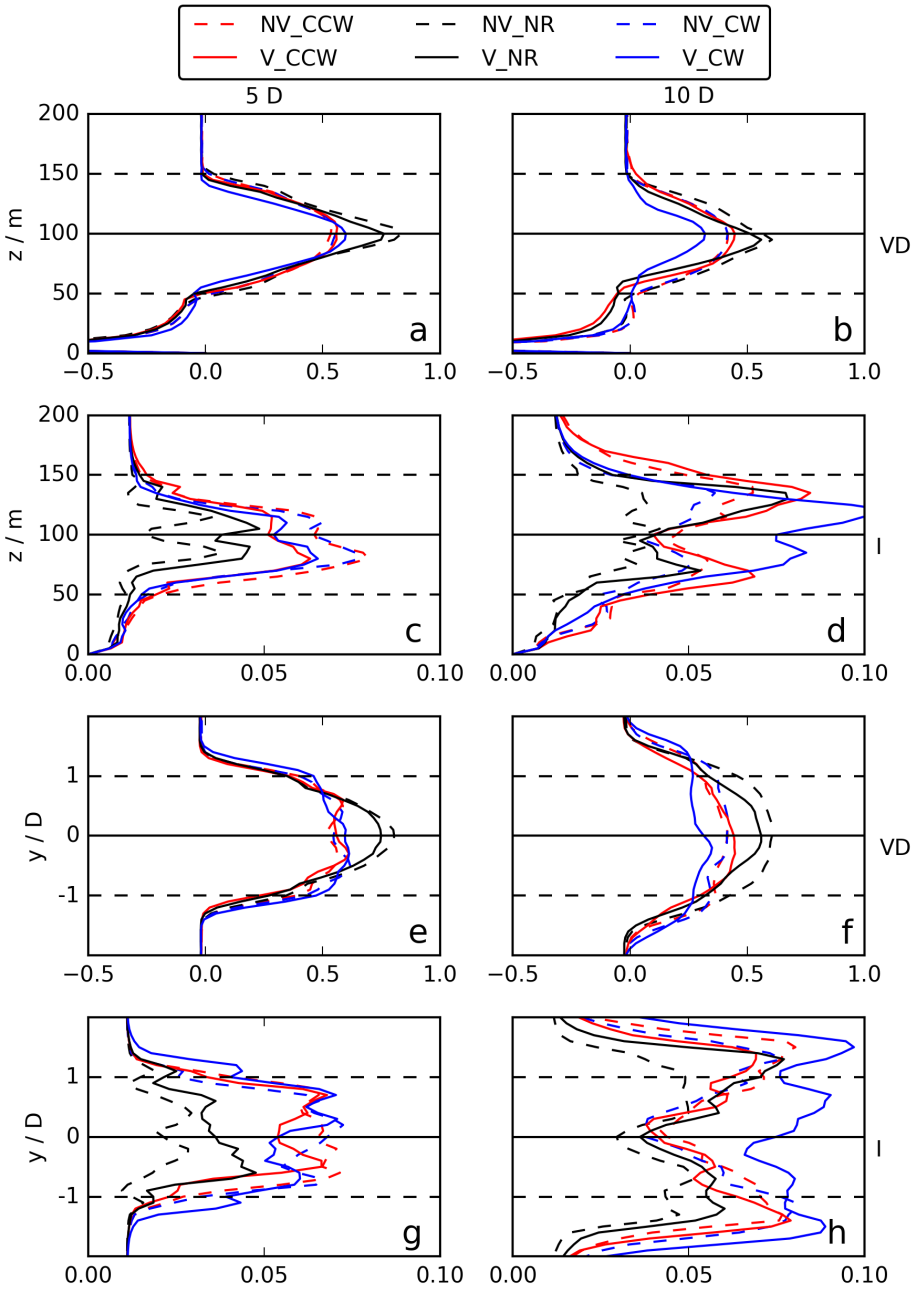

Figure 4. Vertical profiles of the velocity deficit in a, b and the turbulent intensity in c, d and the corresponding spanwise profiles in e, f, g, and h at two downstream distances of 5 D (first row) and of 10 D (second row), each through the centre of the rotor disc.

C. Analytical modeling

C1

Eq(9): Why 0.3? Could you provide a physical justification for using 0.3? This value can be related to the induction factor of the turbine, but, in the current form, it is not justified.

It is motivated on page 15 line 12 (original manuscript). According to Fig. 4, the maximum value of the velocity deficit is roughly 0.7, resulting in the factor 0.3 used in Eq. 9.

The calculation of the velocity deficit

$$VD_{i,j,k} \equiv \frac{\overline{u_{1,j,k}} - \overline{u_{i,j,k}}}{\overline{u_{1,j,k}}}. \tag{2}$$

is directly related to the axial induction factor

$$a = \frac{V_\infty - V_R}{V_\infty} \tag{3}$$

following Manwell et al. (2002) and Hansen (2008), resulting in a value of 0.3=1-a in the calculation of the axial force as used in momentum theory.

We added the comparison with the axial induction factor and momentum theory in the paper as:

'We apply a fraction of 0.3, which can be related to $VD_{max} = 0.7$ of the rotating disc simulations in Fig. 4 and consequently to an axial induction factor a of 0.7, resulting in a fraction of 0.3 = (1-a), as it would be the case by calculating the axial force with momentum theory Manwell et al. (2002); Hansen (2008).'

Further, we modified the definition of u_M to make it more straight-forward. We changed from

$$u_M(r, x_{pos}) = 1.3 \cdot u_{BL} \left(\frac{x_{pos}}{x_{rec}} \right)^\gamma \tag{4}$$

to

$$u_M(r, x_{pos}) = u_{BL} - 0.3 \cdot u_{BL} \left(\frac{x_{rec} - x_{pos}}{x_{rec}} \right). \tag{5}$$

This results in an even better fit of $\overline{u}$ in Fig. 6 in comparison to 5, however, with no relevance for the important components of v and w.

C2

Eqs (13) and (14): This assumption should be verified or assessed by comparing the model to the simulation results. It is known that the lateral and vertical components of the velocity in the wake are different from the incoming wind.

The comparison is presented in Fig. 12.

The difference in the wake from the incoming wind is considered by including v_{WT} and w_{WT}. We added in the text: 'From a linear superposition of the boundary layer flow with the wind-turbine induced forces on the flow field results for the developed

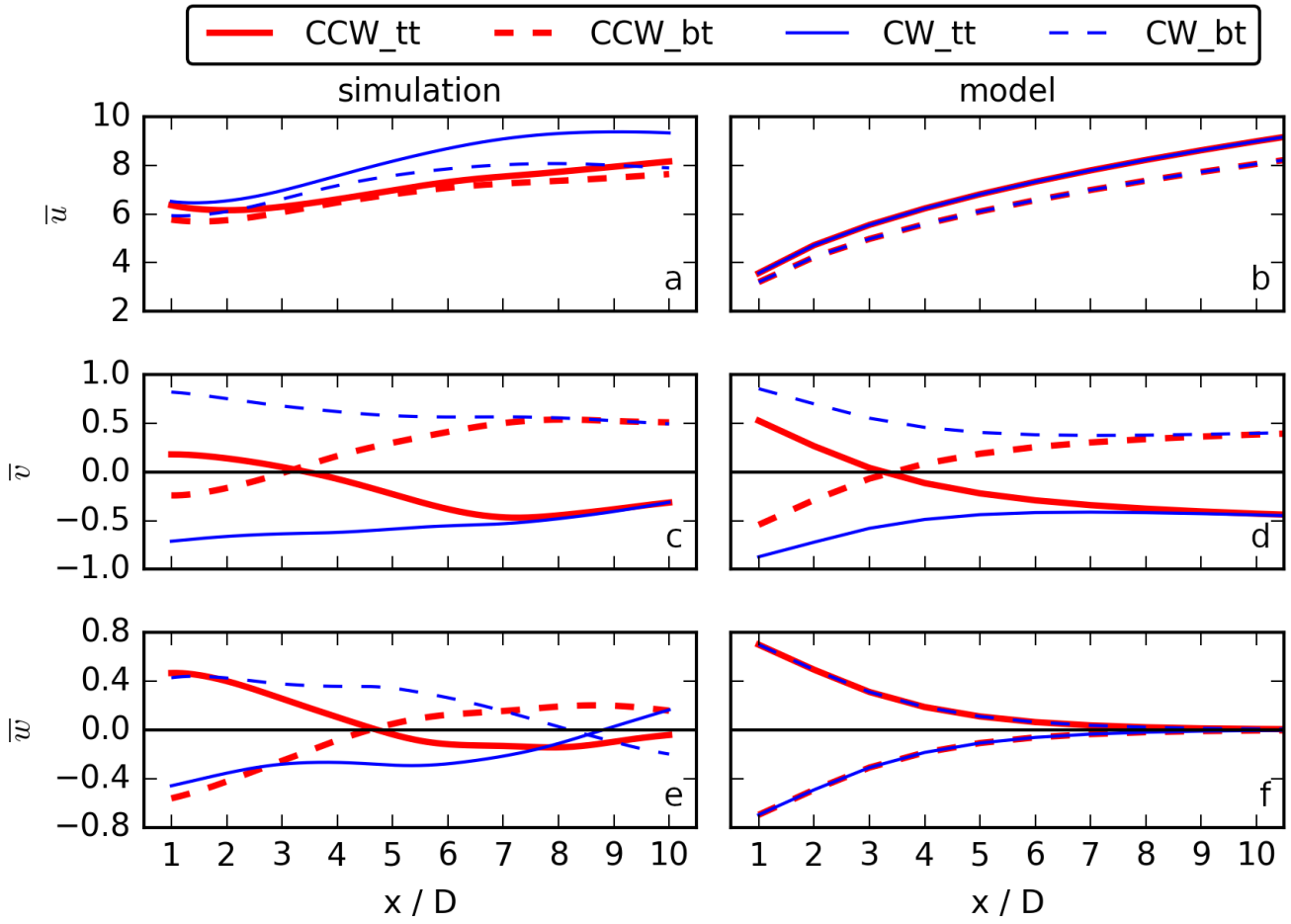

Figure 5. Sector averages $\overline{u}$ in (a), $\overline{v}$ in (c), and $\overline{w}$ in (e) for the veered cases V_CCW and V_CW. $\overline{u}$ and $\overline{v}$ show the top-tip and bottom-tip sectors, $\overline{w}$ the right (solid line) and left (dashed line) sectors. The corresponding model components are shown in (b) for $\overline{u}$, (d) for $\overline{v}$, and (f) for $\overline{w}$.

simplified wake model (M):'

Further, we are aware of the fact that our simplified model does not include any non-linear entrainment processes etc., however, as its aim is only to explain the differences in the v and w components, this simplification is considered to be appropriate.

C3

I could not follow how Eqs. (18-20) are obtained from Eqs. (15-17). Eqs. (15-17) are only a function of r. However, Eqs. (18-20) are a function of r and x.

Eqs. (15-17) (no 16-18) only depend on the radial position. Now, the downstream behaviour is included in Eqs. (18-20) (now

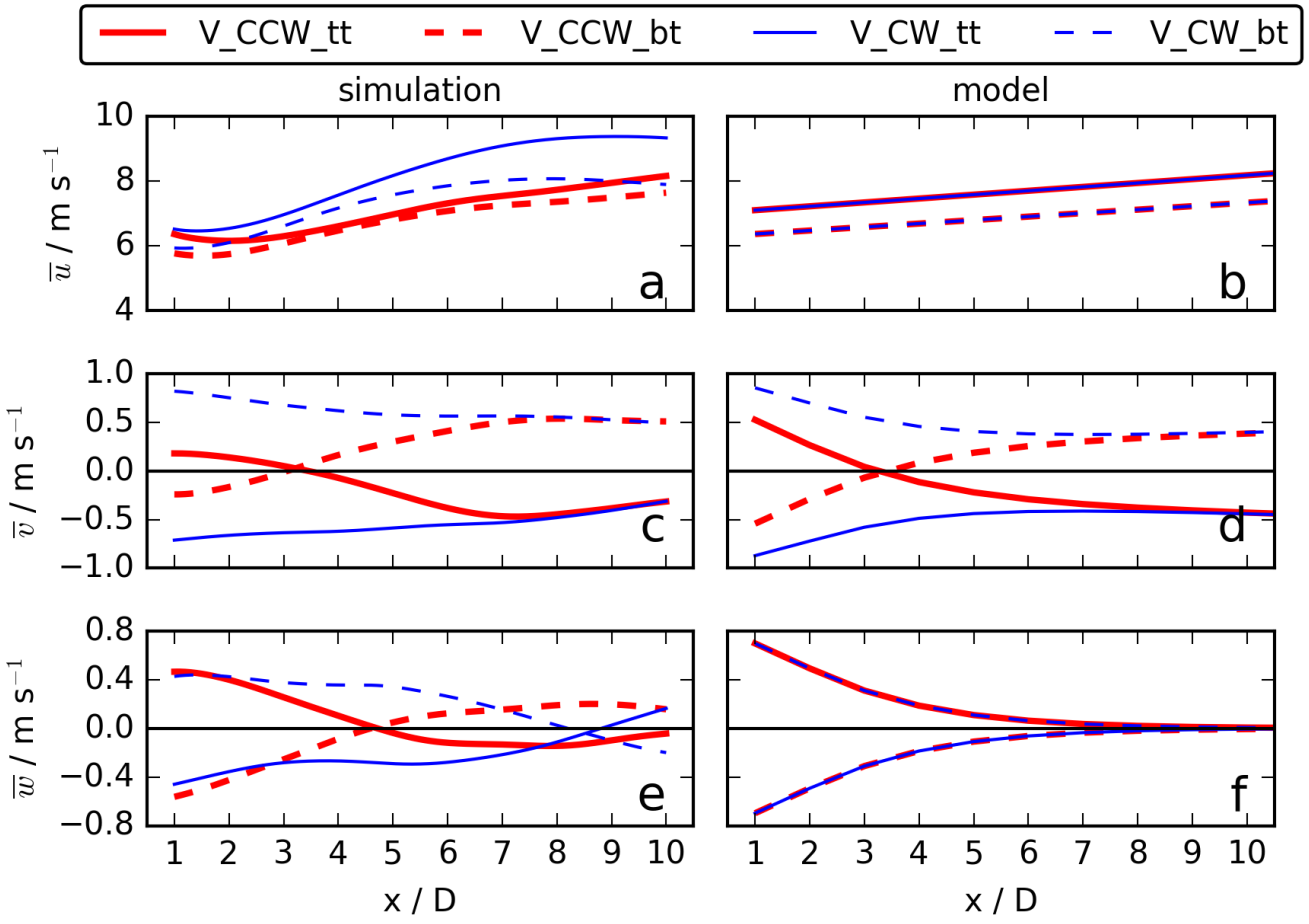

Figure 6. Sector averages $\overline{u}$ in (a), $\overline{v}$ in (c), and $\overline{w}$ in (e) for the veered cases V_CCW and V_CW. $\overline{u}$ and $\overline{v}$ show the top-tip and bottom-tip sectors, $\overline{w}$ the right (solid line) and left (dashed line) sectors. The corresponding model components are shown in (b) for $\overline{u}$, (d) for $\overline{v}$, and (f) for $\overline{w}$.

19-21). Here, approaching downstream, the u, v, and w components increase due to wake recovery. The v and w components are also affected by the rotational direction of the ambient flow. The way of including the downstream position is explained by 1. and 2. on page 19. Therefore, now Eqs. (19-21) are a function of the radial position in relation to the rotor center and likewise on the downstream distance from the rotor. Therefore, with Eqs. (19-21) an assumption at each waked grid point is possible.

Also, it should be explained how the magnitude of δ and γ are obtained.

The magnitude of γ and δ result from archiving the best possible agreement between the model results and the simulation results (e.g. see Fig. 12). We added: 'The values of γ and δ are determined by empirical fitting.' We consider empirical fitting appropriate, as the values of δ and γ only modify the amount of v and w downwind, however, not the sign of both.

C4

Does the proposed model satisfy basic physics like mass and momentum conservation? This point needs to be clarified in the text.

Conservation of mass: Considering Eqs. 18-20,

$$u_M(r, x_{pos}) = u_{BL} - 0.3 \cdot u_{BL} \left(\frac{x_{rec} - x_{pos}}{x_{rec}} \right) \tag{6}$$

$$v_M(r, x_{pos}) = \left(v_{BL} \pm (\pm \omega r \frac{r}{R} cos(\Theta)) \left(\frac{1}{exp \frac{x_{pos}}{x_{fad}}} \right)^{\delta} \right) \left(\frac{x_{pos}}{x_{rec}} \right)^{\gamma} \tag{7}$$

$$w_M(r, x_{pos}) = \pm (\mp \omega r \frac{r}{R} sin(\Theta)) \cdot \left(\frac{1}{exp \frac{x_{pos}}{x_{fad}}} \right)^{\delta} \cdot \left(\frac{x_{pos}}{x_{rec}} \right)^{\gamma}, \tag{8}$$

and the continuity equation. Considering a certain position x_{pos}, from Eq. 6 follows $\frac{\partial u}{\partial x} = 0$. Further, considering $r^2 = y^2 + z^2$, $\frac{\partial v}{\partial y} \approx constant * y$ and $\frac{\partial w}{\partial z} \approx constant * z$. Therefore, form the continuity equation follows y+z=0. This can be interpreted as a conservation of mass on concentric circles around hub height. This is in agreement with the development of the model, which was assumed to be radially symmetric to the nacelle. Considering complex entrainment processes, we think the mass has not to be conserved at specific downstream regions, as it is the case over the whole domain.

Conservation of momentum:

This is verified as the model is constant in time and, no temporal changings are expected. Further, the model is linear, therefore no advection, only Coriolis force and pressure gradient force (no pressure change) are present.

References

Englberger, A. and Dörnbrack, A.: Impact of the diurnal cycle of the atmospheric boundary layer on wind-turbine wakes: a numerical modelling study, Boundary-layer meteorology, 166, 423–448, https://doi.org/10.1007/s10546-017-0309-3, 2018a.

Englberger, A. and Dörnbrack, A.: A Numerically Efficient Parametrization of Turbulent Wind-Turbine Flows for Different Thermal Stratifications, Boundary-layer meteorology, 169, 505–536, https://doi.org/10.1007/s10546-018-0377-z, 2018b.

Englberger, A. and Lundquist, J. K.: How does inflow veer affect the veer of a wind turbine wake?, in: North American Wind Energy Academy 2019 Symposium, Virginia Tech, 2019.

Englberger, A., Lundquist, J., and Dörnbrack, A.: Should wind turbines rotate in the opposite direction?, to be submitted, 2019.

Hansen, M. O.: Aerodynamics of wind turbines, vol. 2, Earthscan, London and Sterling, UK and USA, 181 pp, 2008.

Manwell, J., McGowan, J., and Roger, A.: Wind Energy Explained: Theory, Design and Application, Wiley: New York, NY, USA, 134 pp, 2002.